IEEE Access
Multidisciplinary ⋮ Rapid Review ⋮ Open Access Journal

Received November 3, 2021, accepted January 10, 2022, date of publication January 25, 2022, date of current version March 9, 2022.

Digital Object Identifier 10.1109/ACCESS.2022.3145965

Droop Control Optimization Strategy for Parallel Inverters in a Microgrid Based on an Improved Population Division Fruit Fly Algorithm

XINKUN TAO, LI ZHANG, AND FUZHONG WANG
School of Electrical Engineering and Automation, Henan Polytechnic University, Jiaozuo, Henan 454003, China

Corresponding author: Li Zhang (dqzhangli@hpu.edu.cn)

This work was supported in part by the National Natural Science Foundation of China under Grant U1804143, in part by the Technology Planning Project of Henan Province of China under Grant 202102210295, in part by the Fundamental Research Funds for the Universities of Henan Province under Grant NSFRF210424, in part by the Doctoral Scientific Research Foundation of Henan Polytechnic University under Grant B2017-20, and in part by the Young Key Teacher Program of Henan Polytechnic University under Grant 2019XQG-17.

ABSTRACT When the microgrid topology changes, the traditional droop control strategy affects the dynamic performance and steady-state accuracy of the inverter. To this end, this paper is based on an improved population division fruit fly algorithm. An optimization strategy for grid-connected inverter droop control is proposed in this paper, and then, the PI parameters of microgrid droop control are optimized in real time. This strategy divides the fruit fly population into three zones according to the inverter output and then automatically updates the multistrategy mode according to the difference in fruit fly performance in each zone. Among them, in zone I, a local fine search is conducted to ensure that the population does not degenerate; in zone II, adaptive adjustment is performed, ensuring the diversity and convergence of the algorithm; and in zone III, fruit flies are guided to accelerate convergence. The effectiveness and feasibility of this strategy is verified by this article according to simulation experiments and actual application cases. The results show that the proposed control strategy can make the inverter output follow the changes in the system for adaptive adjustment. The inverter response speed is increased 40-fold, and the steady-state error is reduced by 4.3%.

INDEX TERMS Improved fruit fly optimization algorithm, population division, multistrategy, adaptive, droop control, online optimization.

I. INTRODUCTION

Microgrid droop control is a double closed-loop control system formed by multiple proportional integral (PI) controllers in series and in parallel. When the system topology changes, the conventional PI controller cannot adapt to changes in the system parameters. Conventional PI controllers decrease inverter response speed, and the output power, frequency, and voltage of the inverter cause problems such as being over the limit and oscillation. The dynamic performance and steady-state accuracy of droop control are affected. Therefore, the real-time tuning of PI parameters is required online.

The current control strategy that realizes the parallel operation of microgrid multimachines in island mode is dominated by droop control, the principle of which is to realize load power distribution according to capacity by adjusting the characteristic curve with difference [1]. Many scholars have conducted much research on the issues related droop control. Droop-control improvement methods can be roughly divided into two categories: the model simplification of complex systems and the introduction of intelligent algorithms into complex systems. The model simplification of complex systems. The P-U droop control model based on a PI controller was designed by [2]. This method simplifies the model, analyses the steady-state and dynamic performance of the system, and uses the sequential method to determine the control parameters so that the voltage deviation is reduced. A new droop control current-sharing strategy based on equivalent impedance difference control was proposed by [3], and the dq-axis model of the AC/DC rectifier and its equivalent circuit were analysed. The results show that this method not only reduces the bus voltage attenuation but also achieves

The associate editor coordinating the review of this manuscript and approving it for publication was Yongming Li.

current sharing. In the work of [4], through circuit steady-state analytical equations, a bus voltage stabilized secondary compensation autodisturbance-rejection controller was designed, and this method suppressed the line impedance voltage drop and load power disturbance. However, today's control system is a dynamic and complex nonlinear control system. Moreover, it is difficult to simplify the model and derive the formula [5]. The introduction of intelligent algorithms into complex systems. [6] used a heuristic artificial bee colony algorithm to tune PI parameters, and verified the effectiveness of the proposed strategy by designing different scenarios, and realized power redistribution. [7] aimed at the I-V droop control strategy, proposing an adaptive PI controller. This strategy used a compromise method to select PI parameters based on response speed and steady-state performance so that droop control exhibited improved dynamic performance. The strategy of particle swarm optimization (PSO) droop control PI parameters was proposed by [8]. This strategy is compared with traditional PI droop control and has better dynamic performance, as was verified by experiments with different load disturbances. The strategy of the grasshopper optimization algorithm (GOA) for droop control PI parameters was proposed by [9]. In the photovoltaic microgrid system, this optimization strategy minimized the overshoot of the current, voltage and frequency output by the inverter, as well as the minimum total harmonic distortion (THD). The online optimization strategy of voltage source inverter (VSI) PI parameters based on the fruit fly algorithm was designed by [10]. This strategy took the minimum integral time absolute error (ITAE) value of the PI error as the goal and optimized the four PI controls in the system simultaneously so that the performance of the PI controller was enhanced. However, the strategy did not consider the fluctuation in voltage and frequency. The use of different algorithms to optimize droop control parameters was proposed by [11] and [12]. This method suppressed voltage and frequency fluctuations. At present, although most scholars have proposed many improvement methods, they have not considered the adaptive capability of droop control system inverters when the microgrid topology changes.

In practice, the microgrid is a dynamic system, and the wind and solar abandonment phenomenon caused by the uncertainty of renewable power output and load demand often occurs [13]. Therefore, the microgrid performs not only load switching but also microsource switching. Microsource switching causes the microgrid system structure to change, and the PI parameters must then be retuned. In the above algorithm comparison, the fruit fly algorithm has the characteristics of fast optimization speed, simple structure, low-level calculations, adjustable parameters, outstanding global search ability, and strong solving ability for nonlinear problems [14], [15]. Therefore, many scholars have applied the fruit fly algorithm to the optimization of microgrid parameters. The standard fruit fly algorithm has outstanding global optimization capabilities in the early stage and can quickly find the optimal value, but later search capabilities are poor and the optimization accuracy is not high when solving complex problems [16]. This feature was pointed out by [17]. With the increase in the number of microsources, it is necessary to improve the exploration and exploration capabilities of fruit fly algorithms to ensure optimization accuracy and speed. The current improvements to the FOA algorithm are mainly divided into two categories: (1) Increase population diversity, the sentinel mechanism and multigroup mechanism were introduced by [18]. The sentinel mechanism consists of greedy selection and Gaussian variation to enhance the convergence speed of the algorithm. The multigroup mechanism divides the fruit fly population into several subgroups to enhance the exploration ability of fruit flies. A double driven fruit fly algorithm was proposed by [19]. In this framework, fruit fly flight is guided by the concept of multiple repellents and attractants. Adaptive determination of the search radius is performed. The algorithm is used to optimize and enhance the performance of the PID framework. (2) Increase population convergence, a fruit fly algorithm for adaptive cloud escape search was proposed by [20]. The search method considered the number of iterations as the guiding factor to adjust the global and local search. Moreover, a new evolutionary direction intelligent selection mechanism was proposed by [21]. This selection mechanism provides the correct direction for fruit flies, and the convergence speed of the algorithm is increased. An improved fruit fly optimization algorithm (IFOA) was proposed by [22], by introducing the inertial weight function to the search step, the search ability of the algorithm was improved. In the past improvements, only the unilateral performance of the fruit fly population was often considered, making the overall performance not outstanding. Some scholars have improved the search mechanism of fruit fly vision and smell to improve the search ability of fruit fly algorithms. An improved fruit fly optimization algorithm based on double strategies co-evolution was proposed by [23]. One of the two carefully constructed evolutionary strategies was randomly selected as the olfactory search operator of the current individual according to probability. Thus the olfactory search mechanism of the hybrid coevolution of the two strategies was formed. This mechanism can reasonably balance the global exploration and local exploitation of the algorithm. An improved fruit fly optimization algorithm was proposed by [24], through the construction of hybrid learning olfactory search strategy, the global exploration and local exploitation of the algorithm were effectively enhanced and reasonably balanced. A hybrid fruit fly optimization algorithm was proposed by [25]. the traditional fruit fly optimization algorithm is improved by using the multi-swarm co-evolution feature, and a hybrid fruit fly optimization algorithm with internal and external search strategies is designed. An adaptive multiple neighborhoods collaborative search-based fruit fly optimization algorithm (AMNCS-FOA) is proposed by [26], in the visual search stage, to improve the global search ability of the algorithm, the iterative search is performed with a certain probability to accept the inferior solution as the population center. There is

no real-time feedback of the optimization effect of the fruit fly algorithm in the improved method, and thus the convergence and diversity of the algorithm cannot be balanced, which makes the algorithm perform a large number of invalid calculations. A method of adaptively adjusting the convergence and diversity of the algorithm is proposed, which makes the algorithm more intelligent, and still maintains strong exploration and exploration capabilities when solving various complex problems.

Therefore, to improve the adaptive ability of the inverter of the microgrid droop control system, this paper analyses the basic principles of droop control and the deficiencies of the standard fruit fly algorithm. A population division multistrategy adaptive fruit fly optimization algorithm (MSAD-FOA) is proposed. This strategy can detect and feedback the optimization effect and adjust the PI parameters in real time. The main contributions of this paper are as follows. This paper proposes the concept of population partition, which divides fruit flies into different regions according to their performance. A multi-strategy update mode is proposed. fruit fly with different performance adopts different update strategies, which fully utilizes the exploration and exploration ability of each fruit fly and avoids ineffective calculations. (2) The average individual increment (AII) evaluation index of the fruit fly population proposed in this paper can feed back the effect of algorithm optimization in real time and then adaptively adjust the convergence and diversity of the algorithm. (3) Introducing the absolute value integral term of error derivation into the objective function of microgrid online optimization effectively suppresses the oscillation and deviation of the inverter output power. (4) In non-initial optimization, the use of adaptive and optimal delivery strategies shortens the online optimization time.

This paper is organized as follows. Section II mainly writes the preliminary research on the optimization of droop control strategy based on the fruit fly algorithm, and analyzes the problems existing in the preliminary research. Section III mainly writes the ideas and processes of improving the fruit fly algorithm. In Section IV, the objective function and optimization process of MSAD-FOA optimization droop control strategy are mainly written. Section V is the simulation verification and experimental verification. Section VI mainly writes the contribution of this paper.

II. IDEAS FOR IMPROVEMENT

A. STANDARD FRUIT FLY ALGORITHM

The Fruit Fly Optimization Algorithm is a new algorithm proposed by imitating the food-seeking behavior of fruit flies, think of each problem to be optimized as a fruit fly searching for food in j-dimensional space. Giving the current position of each fruit fly in j-dimensional space $X_i = (X_{i,1}, X_{i,2}, \ldots, X_{i,j})$, $Y_i = (Y_{i,1}, Y_{i,2}, \cdots, Y_{i,j})$ and the flight distance of the fruit fly. Calculated by the adaptability function, then evaluated for each fruit fly. Contribute the fruit fly with the best flavor concentration in the group to the next group, iterate sequentially until the end and output the optimal value. When the Fruit Fly Optimization Algorithm is calculated at the (k+1) iteration, to update the position of fruit fly according to equation (4).

$$\begin{cases} X_{i,j}(k+1) = X_{i,j}(k) + c \cdot L \cdot rand() \\ Y_{i,j}(k+1) = Y_{i,j}(k) + c \cdot L \cdot rand() \end{cases} \tag{1}$$

In equation (1): L for superior step length. c is a non-negative acceleration constant, rand() is a random number which randomly generated between 0 and 1s. i is the number of fruit flies, j is the dimension. $X_{i,j}(k)$, $Y_{i,j}(k)$ are the global optimal position, $X_{i,j}(k)$ and $Xgbest^t_{i,j}$ mentioned below are the same value.

According to the above update equation, the next update iteration of the standard Fruit Fly Optimization Algorithm is the expansion of Fruit Fly population within fixed range, which based on the global optimal value. Thus the standard Fruit Fly Optimization Algorithm has the following problems: ① Only the global optimal experience is considered for each update, but ignores the individual flight experience of fruit fly. ② Fruit Fly population retain only the globally optimal individuals after searching for targets, and then perform a single location update strategy, ignore the flight experience of the entire Fruit Fly population to guide the next iteration of the update. ③ Population convergence and diversity are not detected and parameters cannot be adjusted adaptively. ④ The fixed-step search approach does not take into account the large area search in the early stage and the small area depth search in the later stage.

B. PROBLEM IDENTIFICATION

The droop control strategy is similar to the primary frequency modulation of the generator, and this strategy changes the output power of the inverter by adjusting the grid voltage and frequency. The principle of optimizing the PI parameters of droop control is to establish the corresponding objective function and then use intelligent algorithms to optimize the parameters of the PI controller. In recent years, optimization technology has continued to develop. Intelligent optimization algorithms represented by PSO and genetic algorithms have provided strong technical support for solving complex nonlinear problems. However, when using the PSO and genetic algorithms to optimize the droop control PI parameters, multiple attributes must be updated; however, the calculation process is relatively complicated, and the program is difficult to implement. In comparison, the fruit fly algorithm update strategy is simple, easy to implement, has a low level of calculation, and is more suitable for real-time online optimization.

In the preliminary research, after a large number of experiments, it was found that the FOA-based droop control optimization strategy has the following problems: (1) it causes the inverter's response speed to be slow, and the error is larger in the steady state Fig. 1-(a). The reason for this is that the algorithm cannot adaptively adjust the convergence and diversity. When the algorithm falls into the local optimum, the diversity

cannot be increased, and the algorithm cannot be jumAped out of the local optimum. Therefore, the optimal PI parameters have not been found to ensure microgrid performance. (2) When there are many microsources, the FOA cannot guarantee that each microsource can work normally, and the output power of the inverter fluctuates greatly. The reason for this is that the algorithm's exploration ability is insufficient when the solution dimension increases. (3) The optimization result of the FOA cannot be improved by adjusting the algorithm step size and number of iterations Fig. 1-(a) and Fig. 1-(b). The reason for this is that the exploration and exploration capabilities of the algorithm cannot be effectively improved by changing the step size and number of iterations. (4) By observing the convergence curve of the FOA, it is found that the algorithm can achieve convergence accuracy only after more than 80 iterations. With the increase in the number of microsources, the dimensionality of the algorithm solution is also increased, the FOA has a cliff-like convergence in the optimization process Fig. 1-(c), the convergence of each iteration cannot be guaranteed, and the convergence of the FOA cannot be changed by increasing the number of fruit flies. The reason for this is that the algorithm performs a large number of invalid calculations, which do not contribute to convergence.

C. IMPROVEMENT PROCESS

Through the above analysis and combined with the droop control principle, it can be seen that PI control plays a vital role in droop control and that PI parameters directly influence the control effect. However, the standard fruit fly algorithm cannot accurately calculate the PI parameters when faced with complex systems, so an improved FOA is proposed, the process of which is shown in Fig. 2. Based on the innovation of three partitions, multiple strategies and self-adaptation, this paper improves the algorithm into a closed-loop control algorithm that can detect the optimization effect in real time. In the target search, the algorithm can adaptively adjust the fruit fly population and explore and develop in an optimal way, expanding the scope of population exploration; increasing the population diversity at the same time can accelerate population convergence, taking into account the diversity and convergence of the fruit fly population. The improved FOA, in this article, is called the population division multi-strategy adaptive fruit fly optimization algorithm (MSAD-FOA).

Fig. 2 shows that the main purpose of the improvement is to improve the convergence accuracy and convergence speed of the fruit fly algorithm, the main tasks of which are as follows: (1) improve convergence accuracy by: a) adopting the update method of variable step size; b) introducing the best individual flight experience for the fruit fly into the updated formula and (2) improve convergence speed by: a) adopting the idea of dividing the fruit fly population into three regions, adopting different update strategies for fruit flies with different performances, and giving full play to the optimization ability of each fruit fly; and b) detecting and feedbacking the optimization effect in real time, forming a closed-loop control system, and making negative feedback adjustments to the algorithm in time to avoid invalid calculations.

According to the improved process in Fig. 2, combined with the droop control principle, a diagram of an optimized droop control system based on the MSAD-FOA is obtained, as shown in Fig. 3. The droop control strategy includes double closed-loop control of voltage and current, which is a type of decoupling control of active and reactive power. In the event of a sudden load change, the double closed loop of voltage and current can control the inverter so that it tracks the load power and control the voltage and current so that they are stable.

According to Fig. 3, in droop control, the difference between the given reactive power and the actual reactive power is adjusted by n to obtain the d-axis voltage, and the difference between the reference active power and the actual active power is adjusted by m to obtain the q-axis voltage [27]. Then, the difference between the actual voltage and the given voltage is sent to the PI controller (PI parameters are set by the fruit fly algorithm), and the reference value of the current inner loop control is obtained through the adjustment of the outer loop controller. The adjustment formula is as follows:

$$\begin{cases} i_{dref} = C_f(k_p^1 + k_i^1/s)(u_{dref} - u_d) - \omega C_f u_d \\ i_{qref} = C_f(k_q^2 + k_i^2/s)(u_{qref} - u_q) + \omega C_f u_q \end{cases} \tag{2}$$

In Equation (2), u_{dref} and u_{qref} are the reference voltages, u_d and u_q are the instantaneous voltages. k_p and k_i are the proportional and integral parameters of the PI controller, respectively. ω is the grid angular frequency.

In the current inner loop, the difference between the reference value of the current inner loop and the feedback current is adjusted by the inner loop PI controller to obtain the dq-axis voltage, the adjustment formula of which is as follows:

$$\begin{cases} u_d = (k_p^3 + k_i^3/s)(i_{dref} - i_d) - \omega L i_d + u_d \\ u_q = (k_q^4 + k_i^4/s)(i_{qref} - i_q) - \omega L i_q + u_d \end{cases} \tag{3}$$

By establishing the corresponding objective function, intelligent algorithms are used to optimize parameters $k_p^1, k_i^1, k_p^2, k_i^2, k_p^3, k_i^3, k_p^4, k_i^4$ of the four PI controllers in Equations (2) and (3).

III. IMPROVEMENT AND REALIZATION OF THE FOA

A. DIVISION OF THE FRUIT FLY POPULATION

In order to improve the performance of the algorithm, this paper proposes a method of population partition, which divides fruit flies with different performances into different regions, and then proposes a multi-strategy update mode according to the performance of the region. When the two-partition method is used to conduct an experiment, it does

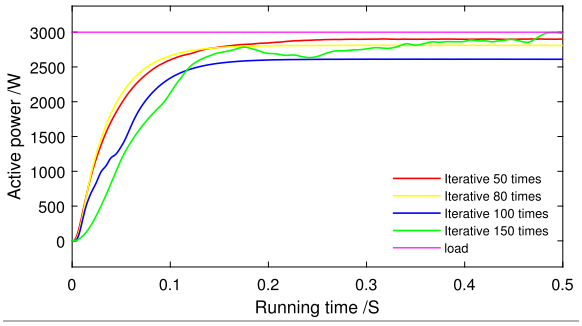

Fig. 1-(a) The optimization result of changing the number of iterations.

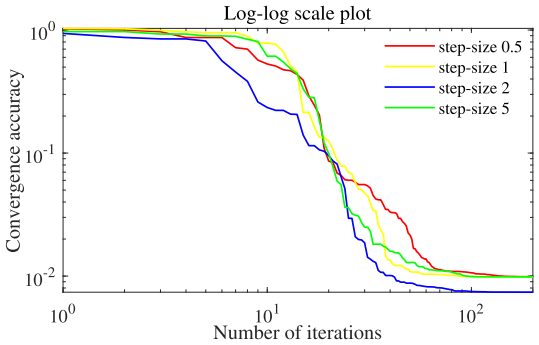

Fig. 1-(b) Optimization results of changing the step size.

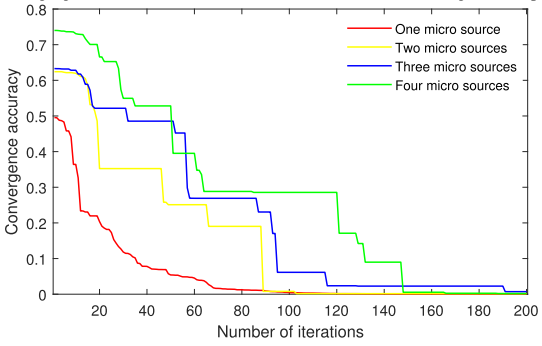

Fig. 1-(c) Optimization results of adding micro source

FIGURE 1. Simulation experiment diagram in the preliminary research.

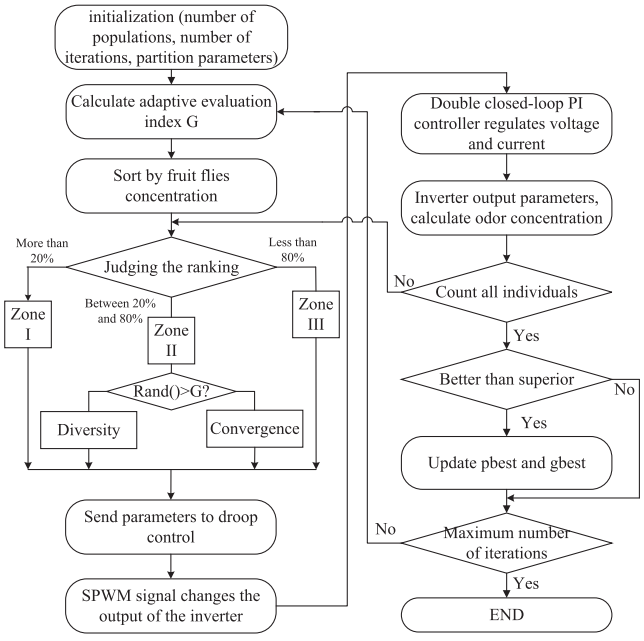

FIGURE 2. Flow chart of improving FOA algorithm to optimize droop control.

not increase the algorithm convergence speed because this method takes into account only a very small number of the best fruit flies, and general performance is not distinguished from poor performance. There is a phenomenon of blurred partitions, and the performance of each fruit fly cannot be fully utilized. When experimenting with a multipartition method, the number of partitions increases. Moreover, the number of fruit flies needs to be increased to ensure that there are a larger number of fruit flies in each area, which leads to a substantial increase in the calculation of the algorithm. Therefore, the partition strategy must not only ensure that fruit flies of different performance levels can be distinguished and avoid the phenomenon of blurred partitions but also consider that increasing the number of partitions could bring with it an enormous amount of calculation. The population division method is proposed in this article according to the characteristics of the partition.

This article takes the optimization minimum as an example. After the algorithm is iterated 5 times, a population division diagram of the population is generated, as shown in Fig. 4. Fruit flies in the population are ranked based on the output performance of the droop control inverter. The population division formula is as follows:

$$region(f(t)) = \begin{cases} I & rank(f(t)) < \alpha \cdot n \\ II & \alpha \cdot n \le rank(f(t)) < \beta \cdot n \\ III & rank(f(t)) \ge \beta \cdot n \end{cases} \quad (4)$$

In Equation (4), α and β are positive numbers between 0 and 1, and n is the number of fruit flies. The fruit fly population is divided into three regions based on the values of α and β, and the number of fruit flies in each region is determined.

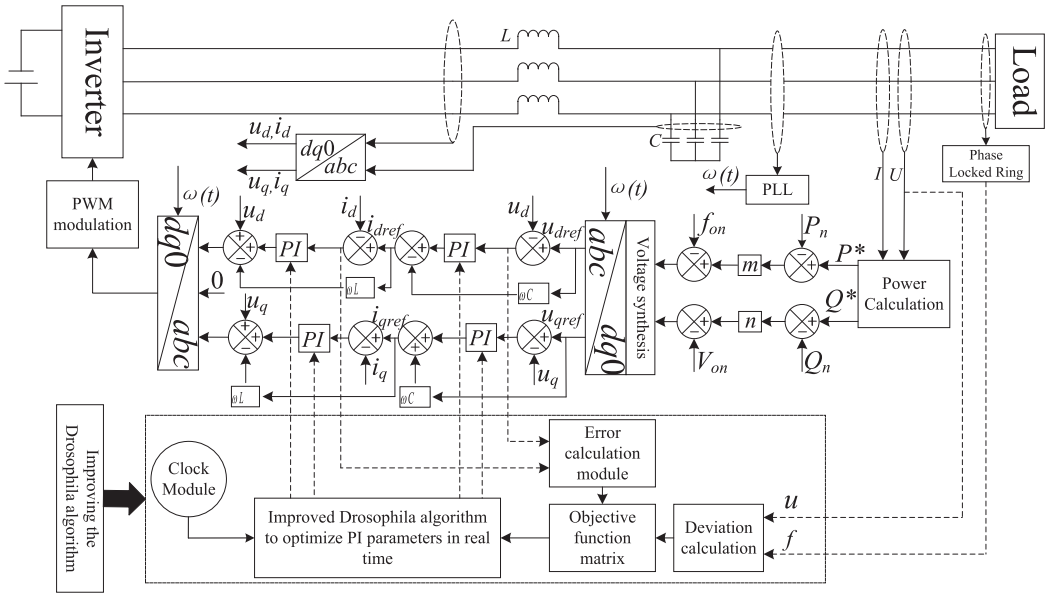

FIGURE 3. Overall structure of the improved fruit fly optimization algorithm for optimal droop control.

B. DETERMINATION OF MULTIPLE STRATEGIES

According to the different performances of fruit flies, different renewal strategies are formulated to enhance the exploration and exploration ability of fruit fly populations.

(1) The fruit flies in **zone I** perform well and are the closest to the optimal target, which shows that the PI parameters in **zone I** optimize the output of the microgrid inverter, and its elite fruit fly population should be maintained. The degradation phenomenon of fruit flies in **zone I** cannot occur, and the local PI parameter search ability should be increased. This paper introduces the concept of historical individual optimality in the fruit fly algorithm by referring to the PSO formula [28]. The updating of PI parameters is jointly guided by the global optimal fruit fly and the individual optimal fruit fly. Then, the updated formula for **zone I** is as follows:

$$\begin{cases} \phi = 1/2 \times (1 + cos(\pi \times \sqrt{\dfrac{t-1}{t_{max}}})) \\ X_{i,j}^{t+1} = X_{i,j}^{t} + \phi \cdot L \cdot (rand_1(Xpbest_{i,j}^{t}) \\ \quad + rand_2(Xgbest_{i,j}^{t} - X_{i,j}^{t})) \\ Y_{i,j}^{t+1} = Y_{i,j}^{t} + \phi \cdot L \cdot (rand_1(Ypbest_{i,j}^{t}) \\ \quad + rand_2(Ygbest_{i,j}^{t} - Y_{i,j}^{t})) \end{cases} \tag{5}$$

In Equation (5), ϕ is the weighting factor, which decreases with the number of iterations. $Xgbest_{i,j}^{t}$, $Ygbest_{i,j}^{t}$ represent the global fruit fly optimal position at time t, and $Xpbest_{i,j}^{t}$, $Ypbest_{i,j}^{t}$ represent the optimal position of the individual fruit fly at time t. This equation shows that for the fruit fly population of **zone I**, the update direction of the fruit fly position at the next moment is always towards the optimal position.

(2) The fruit flies in **zone II** behave normally, which shows that the PI parameters of **zone II** make the output effect of the microgrid inverter normal. However, after a few iterations, the fruit flies in **zone II** can be very close to the optimal target position, making the microgrid output better. In fact, the average fruit flies account for the majority and contain both slightly superior fruit flies and slightly inferior fruit flies. In the process of optimization, these fruit flies serve as "midstream pillars". Therefore, this article does not distinguish the performance of this portion of fruit flies, taking into account, instead, diversity and convergence. The updated formula is as follows:

$$X_{i,j}^{t+1} = \begin{cases} Xgbest_{i,j}^{t} + \phi \cdot L \cdot rand_1, & rand_{i,j} > G \\ X_{i,j}^{t} + \phi \cdot L \cdot rand_2 \cdot (Xgbest_{i,j}^{t} - X_{i,j}^{t}), & \\ \qquad rand_{i,j} \le G \end{cases} \tag{6}$$

$$Y_{i,j}^{t+1} = \begin{cases} Ygbest_{i,j}^{t} + \phi \cdot L \cdot rand_1, & rand_{i,j} > G \\ Y_{i,j}^{t} + \phi \cdot L \cdot rand_2 \cdot (Ygbest_{i,j}^{t} - Y_{i,j}^{t}), & \\ \qquad rand_{i,j} \le G \end{cases} \tag{7}$$

In Equation (6) and (7), G is the evaluation index of population convergence and diversity.

(3) The fruit flies in **zone III** perform poorly; this group of fruit flies makes almost no contribution to the entire fruit fly population and is far away from the optimal target, showing that the PI parameters in **zone III**

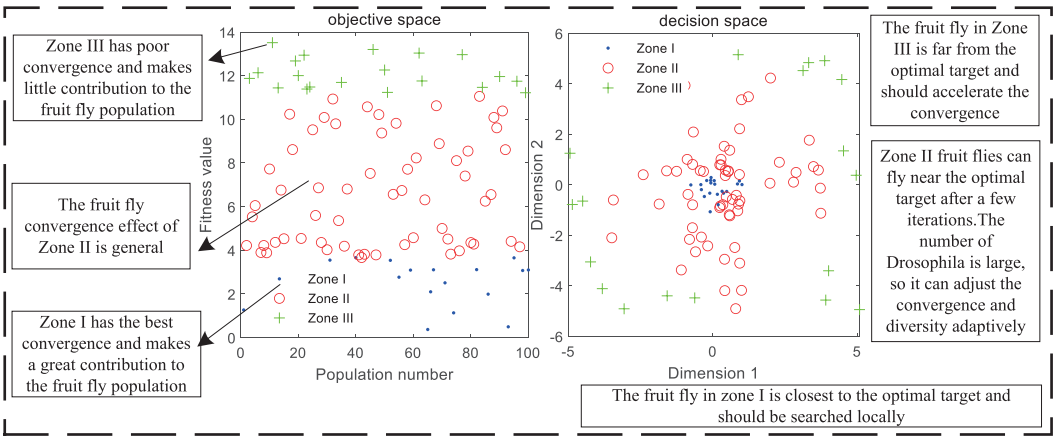

FIGURE 4. Schematic diagram of population zoning.

make the inverter output the worst. The fruit flies in this area should accelerate convergence so that the PI parameters can be quickly updated to a better condition and the output performance of the microgrid inverter can be rapidly enhanced. The updated formula is as follows:

$$\begin{cases} X_{i,j}^{t+1} = X_{i,j}^{t} + \phi \cdot L \cdot (rand_1(Xpbest_{i,j}^{t} - X_{i,j}^{t}) \\ Y_{i,j}^{t+1} = Y_{i,j}^{t} + \phi \cdot L \cdot (rand_2(Ygbest_{i,j}^{t} - Y_{i,j}^{t}) \end{cases} \tag{8}$$

C. IMPLEMENTATION OF THE ADAPTIVE MODE

In algorithms, the convergence and diversity contradict each other to a certain extent. However, adaptively adjusting the convergence and diversity according to the algorithm environment can enhance the comprehensive performance of the algorithm. Some fruit flies are randomly selected from **zone II** to update the convergent position. This update method accelerates the convergence of individual fruit flies and makes the PI parameters rapidly develop in the direction of enhancing inverter output performance. Another group of fruit flies carries out diversity position updates to explore the diversity of PI parameters in line with droop control. In Equation (9), when the random number is greater than G, the first update formula is selected. This update formula is the standard update formula of the fruit fly algorithm. This update formula has a global search capability to ensure population diversity. Otherwise, the second update formula is chosen, the update direction of which is that of the individual fruit fly moving towards the global optimal fruit fly, and the flight distance decreases due to the number of iterations. This update method accelerates the convergence of individual fruit flies. Therefore, the algorithm convergence and diversity can be automatically adjusted according to the adaptive G value. An evaluation index of the AII of the fruit fly population is proposed in this paper as a basis for adaptive adjustment.

$$\begin{cases} DI(t) = \dfrac{1}{n}\displaystyle\sum_{i=1}^{n}\sum_{j=1}^{dim}((X(t)_i^j - Xpbest_i^j) \\ \qquad +(Y(t)_i^j - Ypbest_i^j)) \\ DI(t-1) = \dfrac{1}{n}\displaystyle\sum_{i=1}^{n}\sum_{j=1}^{dim}((X(t-1)_i^j - Xpbest_i^j) \\ \qquad +(Y(t-1)_i^j - Ypbest_i^j)) \\ AII = DI(t) - DI(t-1) \\ G = \eta \cdot AII \end{cases} \tag{9}$$

In Equation (9), $DI(t-1)$ is the dimensional difference between the fruit fly position at the previous moment and the historical optimal position, and $DI(t)$ is the dimensional difference between the fruit fly position at the current moment and the historical optimal position. AII is the increase in the difference in the current moment and previous moment. η is the weighting factor. G is the adaptive adjustment parameter. When the fruit fly updates its position to be near the optimal position, DI decreases. In contrast, when the fruit fly updates its position to be far away from the optimal position, DI increases. A smaller $AII(G)$ means that the fruit fly population is closer to the optimal position of the fruit fly at the current moment compared with that in the previous moment. In this case, the diversity of the fruit fly population should be increased, thereby enhancing the exploitation ability of this population. Similarly, when $AII(G)$ is large, the convergence of the fruit fly population should be accelerated, thereby enhancing the exploratory capabilities of this population. At the same time, the dimensional difference of the position is used for calculation, and the dimensional weighting of the best and worst PI control performance can be carried out to offset the emergence of extreme situations.

D. IMPLEMENTATION STEPS OF THE MSAD-FOA

According to the improvement method of the abovementioned population division, multistrategy, and self-adaptive methods, the optimization steps of the MSAD-FOA are obtained.

Step 1: Initialize the maximum number of iterations, partition parameters, population size and other relevant parameters.

Step 2: Calculate the fitness value of each fruit fly, and update the global optimal position $Xgbest^t_{i,j}$ and $Ygbest^t_{i,j}$ the historical individual optimal position $Xpbest^t_{i,j}$ and $Ypbest^t_{i,j}$ according to Equation (10).

$$IF \quad bestSmell_t < smellbest \begin{cases} Xgbest = X_t(bestIndex) \\ Ygbest = Y_t(bestIndex) \end{cases} \tag{10}$$

$$IF \quad pbest^i_t < smell^i \begin{cases} Xpbest^i_t = X^i_t \\ Ypbest^i_t = Y^i_t \end{cases} \tag{11}$$

Step 3: Calculate the convergence evaluation index of the *AII(G)* of the fruit fly population, rank the values based on the fitness value, and divide the fruit fly population into three zones according to Equation (4).

Step 4: Update the position of the fruit fly according to the different update strategies for different zones, as indicated in Equations (5), (6), (7) and (8).

Step 5: Determine if the algorithm has reached the maximum number of iterations. If the maximum number of iterations has been attained, then output the optimal result; otherwise, repeat steps two through four.

In Equation (10) and (11), $smellbest$ is the global optimal odour concentration, $bestSmell_t$ is the current optimal odour concentration, $pbest^i_t$ is the current individual odour concentration, and $smell^i$ is the historical individual optimal odour concentration. $bestIndex$ is the returned position coordinate.

E. COMPLEXITY OF ALGORITHM CALCULATION

Assuming that the population size is N, the dimension to solve the problem is D, and the number of iterations is T, we can easily get the computational complexity of each part. The computational complexity of fitness value is O(N), the computational complexity of fitness value sorting is O(NlogN) (assuming the quick sort method is used), the complexity of population partition is O(N), and the position of fruit flies is updated. The complexity is O(ND), and the calculation complexity of the adaptive evaluation index is O(ND). The computational complexity of this algorithm is O(NT(2+D+logN)).

Compared with other PSO and GA, the additional computational complexity of the proposed algorithm is mainly due to the proposed multi-strategy and adaptive methods. However, it is acceptable that the significant improvement of optimization benefits bring by the increase of computational complexity(shown in Table 5).

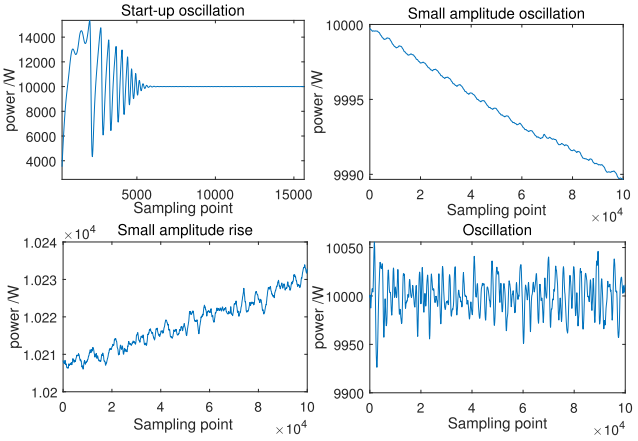

FIGURE 5. Power oscillations and offsets.

IV. ONLINE OPTIMIZATION STRATEGY FOR DROOP CONTROL BASED ON THE MSAD-FOA

A. DETERMINATION OF THE OBJECTIVE FUNCTION

In traditional PI controller optimization, the PI error evaluation performance index $I_{TAE} = \int_0^\infty t \mid e(t) \mid dt$ is often used as the objective function [29]. Considering droop control, the change in the output power is realized by adjusting the frequency and voltage, the stability of which can ensure the stability of active and reactive power. Therefore, the frequency deviation $\triangle f$ and voltage deviation $\triangle u$ are introduced into the objective function. Specifically, $\triangle f = f - f_{ref}$ and $\triangle u = u - u_{ref}$, where $\triangle f$ and $\triangle u$ are the system reference values. The objective function is as follows:

$$\begin{cases} E_1(t) = [\int \mid error \mid dt, \int \mid f - f_{ref} \mid dt, \int \mid u - u_{ref} \mid dt] \\ \theta_1 = [1, 1, 1]^T \end{cases} \tag{12}$$

In Equation (12), $error$ is the error of the PI controller, and θ_1 is the weight matrix of the droop control.

As found in many simulation experiments in the early stage, when Equation (12) is used as the objective function to optimize the microgrid, the result is the unstable output of the microgrid, as shown in Fig. 5. In particular, when the value of the objective function is very small, the output power of the microgrid starts to oscillate, increase slightly, decrease slightly, and then oscillate continuously. This phenomenon is not conducive to the stable operation of the microgrid. In the actual simulation, we found that methods such as increasing the number of algorithm iterations, resetting the initial parameters, and adjusting the step length cannot be revised to effectively suppress this phenomenon. However, we also found that the situation shown in Fig. 5 corresponds to the PI error curve; that is, the change in PI error affects the change in power output. Therefore, as long as it is ensured that the PI error curve does not appear in the situation in Fig. 5, the stable output of the inverter can be guaranteed.

For this reason, the error derivation absolute value integral term is introduced into the objective function $\int \mid \frac{derror}{dt} dt \mid$. When the PI error oscillates or offsets, the value of the objective function continues to increase, and the unstable output is suppressed in the optimization iteration. The new objective function is shown in Equation (13):

$$\begin{cases} E(t) = [\int \mid error \mid dt, \int \mid \dfrac{derror}{dt} \mid, \\ \int \mid f - f_{ref} \mid dt, \int \mid u - u_{ref} \mid dt] \\ \theta = [1, 1, 1, 1]^T \end{cases} \tag{13}$$

B. OPTIMIZATION STRATEGY AND PROCESS

The idea behind optimizing the PI parameters of the microgrid is to convert the online optimization into a mathematical problem by solving the nonnegative minimum of the objective function. In droop control, the PI controller adjusts the outer loop voltage and inner loop current according to the active power and reactive power required by the load. Then, the dq-axis voltage is obtained through the Park change, and a sine wave pulse width modulation (SPWM) signal is generated so that the inverter provides matching active and reactive power to the load and stabilizes the voltage and frequency within the allowable error range. Based on this principle, the MSAD-FOA is applied to the droop control of the microgrid, and the algorithm optimization process is shown in Fig. 6.

When the MSAD-FOA module detects changes in microgrid parameters, the algorithm online optimization process is as follows: (1) the voltage and frequency on the bus are collected through the information acquisition module, and the PI errors of the voltage outer loop and the current inner loop are collected; (2) the weighted calculation module is used to obtain the deviation information; (3) with reference to the interval time of the clock module, the deviation information is fed back into the MSAD-FOA in real time; (4) the MSAD-FOA module divides the fruit fly population into three regions according to the feedback information and adopts a multistrategy adaptive update mode according to the different characteristics of each region, updates the PI parameters, and adjusts the PI parameters in the droop control in time. By doing this, the algorithm enhances the control effect of the voltage outer loop and the current inner loop and improves the output performance of the inverter until the optimization ends.

V. EXPERIMENTAL RESULTS AND ANALYSIS

A. MSAD-FOA VERIFICATION

To test the performance of the proposed algorithm, this paper compares the MSAD-FOA with the FOA [30], PSO algorithm, and genetic algorithm (GA). The test functions are typical unimodal (Sphere, Rosenbrock, Ackley) and multimodal (Rastrigin, Griewank, Schwefel) functions. These six functions have different characteristics and can be used to examine the optimization performance of the algorithm for different types of problems and to verify the convergence speed and accuracy of the algorithm. In the experiment, the number of iterations and population initialization of the four algorithms are all set to 100. The dimensions are set to 2, 5, 8, and 10. Fifty experiments are performed on each dimension to calculate the average value of convergence accuracy (mean) and the standard deviation of the optimal value (std.). The algorithm is realized by MATLAB R2020a.

1) VERIFICATION OF THE VALUES OF PARTITION PARAMETERS α AND β

The convergence and diversity of fruit flies in **zone II** can be adaptively adjusted according to the algorithm environment, so how to determine partition parameters and affects the overall algorithm performance. Fig. 7 shows the change curve of the *AII* evaluation index of and when the proposed algorithm solves the Ackley and Griewank functions. The value schemes are as follows: case 1: $\alpha = 0.1N$, $\beta = 0.9N$; case 2: $\alpha = 0.2N$, $\beta = 0.8N$; case 3: $\alpha = 0.3N$, $\beta = 0.7N$.

Fig. 7 shows that with the increase in the number of fruit flies in **zone II**, the algorithm convergence speed gradually slows down; in contrast, it speeds up the algorithm convergence speed. When the number of fruit flies in **zone II** is large, the range of *AII(G)* change is large, and the fluctuation is more obvious, indicating that the algorithm has large diversity; in contrast, there is small diversity when the number of fruit flies is small. In Fig. 7-(a), in case 3, the number of fruit flies in **zone II** smaller, and *AII(G)* has smaller fluctuations, steep declines, and poor algorithm exploration capabilities. In case 2, the number of fruit flies increases, the range of *AII(G)* changes increases, and algorithm performance is improved. It can also be seen from Fig. 7-(b) that when the number of fruit flies in **zone II** is reduced to a certain extent, the algorithm convergence speed is not increased, but too much of an increase causes the algorithm to converge slowly. To ensure the exploration and exploration performance of the algorithm, the values of the partition parameters α and β in this paper are 0.2 and 0.8, respectively.

Fig. 8 shows the adaptive G-change curve with 6 test functions and 10 dimensions when case2 is selected. Three typical unimodal functions (F1–F3) and three typical unimodal functions (F4–F5) are used (F1-Sphere, F2-Rosenbrock, F3-Ackley, F4-Rastrigin, F5-Griewank, F6-Schwefel). To prevent excessive divergence and convergence of the MASD-FOA, the range of variation of the adaptive G is set between 0.2 and 0.8. The change curve is determined according to the proposed evaluation index of the average individual increment of the fruit fly population. When $G > 0.5$, the diversity of the algorithms is maintained. When $G < 0.5$, the convergence of the algorithm is maintained. As shown in Fig. 8, the algorithm maintains a high diversity in the early stage, and the algorithm maintains a high convergence after fewer adjustments and iterations. Therefore case2 is chosen so that the algorithm has better convergence.

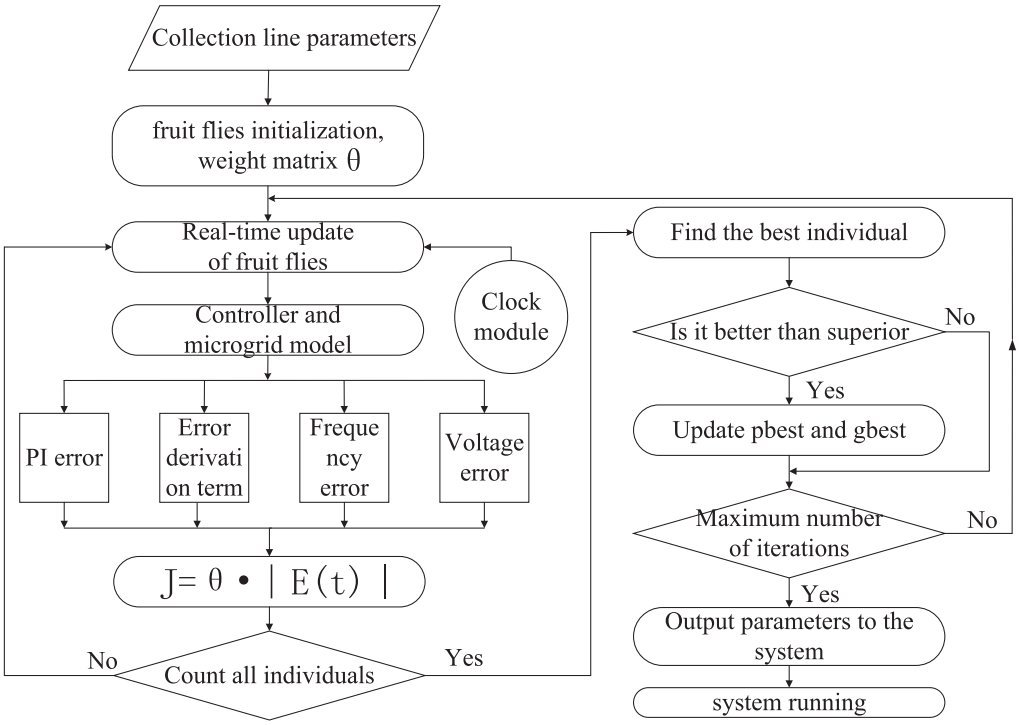

FIGURE 6. Flow chart of droop control algorithm for microgrid inverter based on MSAD-FOA optimization.

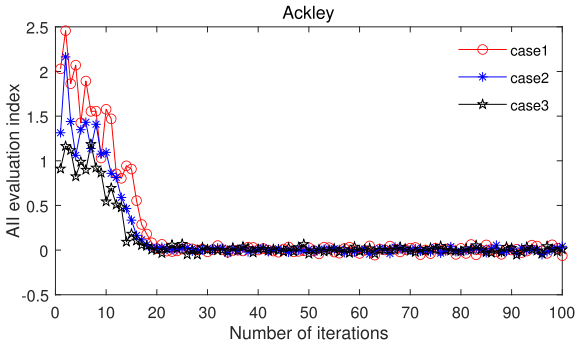

Fig. 7-(a) Optimize Ackley function

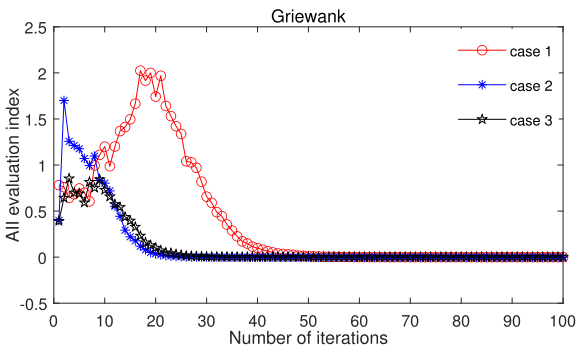

Fig. 7-(b) Optimize Griewank function

FIGURE 7. Changes of AII indicators under different partition parameters.

2) ALGORITHM COMPARISON RESULTS AND ANALYSIS

The experimental results are shown in Table 1 and Table 2. In 24 experiments, the MSAD-FOA achieved the optimal average 21 times, and the optimal standard deviation was achieved 16 times. The optimization effects of the MSAD-FOA are far higher than those of other algorithms.

The Griewank function has the characteristic that the peak shape is undulating and jumping, and higher dimensions can better detect algorithm convergence. Therefore, a 10-dimensional test was performed on the Griewank function to compare the algorithm convergence speed and accuracy. The results are shown in Fig. 9. The 2-D line plot reflects the fastest convergence speed of the MSAD-FOA. The log-log scale plot reflects that the MSAD-FOA has the highest convergence accuracy of all algorithms tested. Based on Fig. 9, the MSAD-FOA converges uniformly, which is caused by the algorithm's adaptive adjustment of its convergence and diversity according to the optimized environment. The multistrategy update mode improves the exploration and exploration capabilities of the algorithm.

B. MICROGRID SIMULATION EXPERIMENT

1) SIMULATION EXPERIMENTAL DESIGN

To verify the effectiveness of the control strategy proposed in this article, this paper builds a microgrid droop control simulation model based on the microgrid experimental platform of a university in Zhengzhou. Simulation experiments

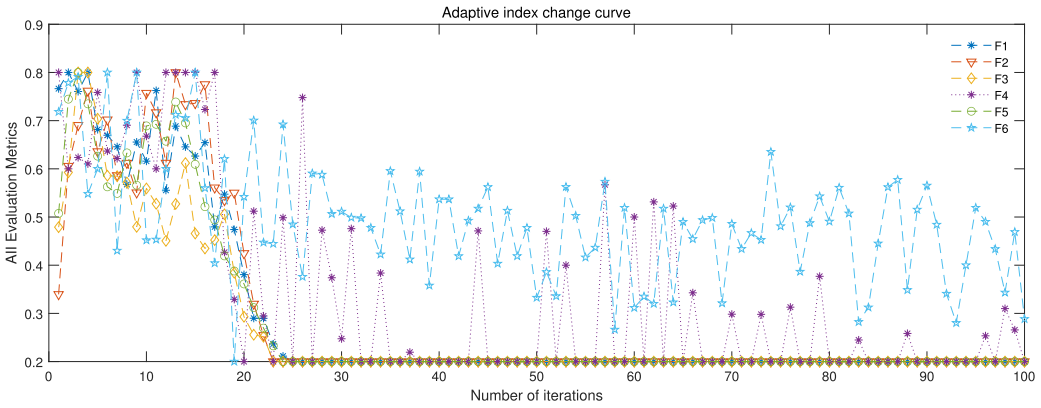

FIGURE 8. Adaptive index change curve.

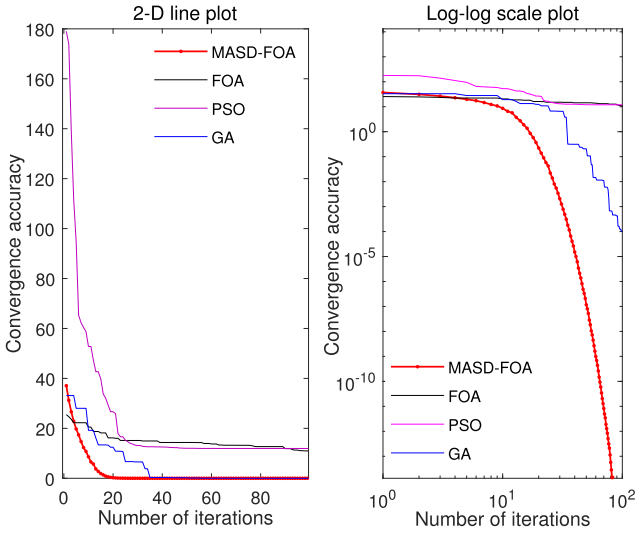

FIGURE 9. Comparison of convergence speed and accuracy of optimized Griewank function.

are performed on the MATLAB/Simulink platform. The operating structure diagram of the microgrid is shown in Fig. 10, and the simulation parameters are shown in Table 3. The line impedance is negligible, and the microgrid operates in an off-grid manner.

2) SIMULATION RESULTS AND ANALYSIS

a: OBJECTIVE FUNCTION VERIFICATION

To verify that the introduction of the PI error derivation absolute value integral term in the objective function can effectively suppress the oscillation and deviation of the inverter power output, microsource 1 runs alone for 0.2 seconds (to more clearly show that the microgrid starts the instant the inverter of the output waveform starts), using the MSAD-FOA to optimize microsource 1, with a load of 3,000 W and 1,000 Var. One uses Equation (12) as the objective function, and the other uses Equation (13) as the objective function. A comparison of the results is shown in Fig. 11 and Fig. 12.

The figure shows that whether is the output is active or reactive power, using the objective function of Equation (13) makes the inverter output power fluctuate slowly in a small range, and the fluctuation range is constant. However, the experiment uses Equation (13) for optimization; there is a large oscillation in the power output when the system is started, and the power output continues to oscillate at a high frequency in the steady state. As the running time increases, the output power gradually becomes stable, but there is still a small deviation.

b: CONTROL EFFECT VERIFICATION

To verify the performance of the MSAD-FOA online optimization PI control strategy, the topology of the microgrid is changed in the experiment. At 0 seconds, microsource 1 works independently; load: 3,000 W, 1,000 Var. After 0.5 seconds, microsources 1 and 2 simultaneously operate with loads of 8,000 W and 3,000 Var, respectively. Equation (13) is used as the objective function. In the experiment, the MSAD-FOA is compared with the FOA, PSO algorithm, GA and traditional methods. Traditional method 1 does not adjust the PI parameters, while traditional method 2 manually adjusts the PI parameters.

Figures Fig. 13 and Fig. 14 are waveform diagrams of the inverter output frequency and voltage. When the microsource is started or the topology changes, the MSAD-FOA is used to make the inverter respond quickly. In terms of frequency, the inverter output is stable, and there is no frequency overshoot. In terms of voltage, the inverter voltage output is stable, without small-scale fluctuations, and the error is very small. The other four algorithms have small oscillations in frequency and voltage. For example, after GA optimization, the microgrid fluctuates greatly at the instant of starting frequency, and the overshoot reaches 0.3 Hz. Although the frequency output performs well after PSO, the output frequency differs greatly from the reference frequency.

TABLE 1. The convergence accuracy of different algorithms and the standard deviation of the optimal value.

Function		2 dim				5 dim			
		MSAD-FOA	FOA	PSO	GA	MSAD-FOA	FOA	PSO	GA
Sphere	Mean	**7.03e-21**	1.87e-04	1.06e-04	1.22e-06	**3.38e-20**	1.01e-03	2.21e-09	3.41e-10
	Std	**4.15e-20**	1.01e-05	1.49e-11	2.18e-07	**2.02e-19**	4.24e-05	6.80e-09	1.51e-15
Rosenbrock	Mean	**7.03e-21**	1.87e-04	1.06e-04	1.22e-06	**3.38e-20**	1.00e-03	2.21e-09	3.41e-10
	Std	9.41e-04	1.10e-03	**6.56e-09**	2.65e-01	1.93e-01	1.70e-01	1.45	1.64e-03
Ackley	Mean	9.56e-11	4.30e-02	2.35e-06	**8.88e-16**	**1.21e-10**	6.70e-02	7.57e-05	2.24e-09
	Std	**1.99e-10**	2.55e-01	5.48e-06	3.88e-09	**3.30e-10**	1.80e-03	1.64e-01	3.06e-08
Rastrigin	Mean	**7.93e-15**	3.79e-2	2.93e-09	1.85e-10	**7.11e-15**	7.22e-03	3.78	5.03e-12
	Std	**0**	3.92e-01	9.95e-03	**0**	**7.11e-14**	1.15	1.78	3.99e-09
Griewank	Mean	**1.01e-16**	6.31e-05	2.01e-08	1.26e-13	**1.11e-16**	2.13e-04	1.55e-02	3.13e-03
	Std	**0**	2.71e-03	3.32e-03	**0**	**0**	1.6e-03	1.15e-02	8.93e-04
Schwefel	Mean	**8.37e+02**	7.48e+02	8.31e+02	1.90e-03	**1.9e+03**	2.04e+03	2.08e+03	2.08e+03
	Std	2.21e-02	5.22e+02	**4.91e-12**	2.95e-01	1.84e+01	7.27e+02	**1.50e-09**	1.74

TABLE 2. The convergence accuracy of different algorithms and the standard deviation of the optimal value.

Function		8 dim				10 dim			
		MSAD-FOA	FOA	PSO	GA	MSAD-FOA	FOA	PSO	GA
Sphere	Mean	**1.69e-20**	2.40e-03	2.31e-07	4.21e-08	**3.31e-19**	3.63e-03	3.12e-06	7.78e-06
	Std	**1.10e-19**	1.33e-04	2.28e-07	8.25e-08	**5.79e-19**	1.86e-06	3.36e-06	4.17e-05
Rosenbrock	Mean	6.85	5.45	**3.31**	6.86	8.22	7.69	**7.23**	8.89
	Std	**1.41e-02**	2.01e-01	2.03	1.68e-01	**8.35e-02**	2.84e-01	1.12e+01	2.52e-01
Ackley	Mean	**1.65e-10**	8.52e-02	2.667e-01	4.93e-04	**6.08e-10**	9.47e-03	6.01e-01	2.50e-03
	Std	**2.53e-10**	2.41e-03	6.67e-01	2.74e-04	**4.33e-10**	2.80e-03	8.05e-01	3.60e-03
Rastrigin	Mean	**1.42e-14**	1.43	8.40	1.49e-04	**1.42e-05**	2.31	1.33e+01	2.01e-02
	Std	3.81e-02	2.37	4.43	**8.70e-03**	6.04e-01	2.67	5.87	**1.04e-01**
Griewank	Mean	**4.28e-08**	3.58e-04	3.17e-02	1.30e-03	**1.78e-14**	4.64e-04	3.09e-02	2.01e-03
	Std	**0**	1.57e-05	3.09e-02	1.92e-03	**1.00e-03**	5.91e-02	2.34e-02	3.91e-03
Schwefel	Mean	**3.15e+03**	3.28e+03	3.33e+03	3.33e+03	4.16e+03	**4.09+03**	4.15e+03	4.16e+03
	Std	2.72e+01	1.34e+02	**1.33e-07**	2.47	3.96e+01	4.74e+01	**5.26e-01**	2.74

TABLE 3. The convergence accuracy of different algorithms and the standard deviation of the optimal value.

Parameter Name	Numerical value	Parameter Name	Numerical value
DC side voltage /V	800	Rated frequency /Hz	50
Filter Inductors /H	1.35×10^{-3}	Rated voltage /V	311
Filter Capacitor /F	50×10^{-6}	Active power droop factor	$1e^{-4}$
Reference active power	3000 W	Reactive power droop factor	$3e^{-4}$
Reference reactive power	0 Var	– – – – –	– –

Fig. 15 is the waveform diagram of the inverter output power. It can be seen from the figure that when the microsource is started or the topology changes, the GA decreases the inverter response speed; the standard FOA makes the inverter steady-state error larger and the response speed slower; and PSO leads to the output power of the inverter oscillating when it is started. However, the MSAD-FOA enables the inverter to respond quickly, with almost no overshoot; can quickly follow the load change; and can ensure the accurate output of the inverter power in the steady state. It can be seen from the partially enlarged view that the MSAD-FOA makes the response state of the inverter a smoothly rising curve, while PSO causes the output power of the inverter to oscillate during startup. It can be seen at 0.5 seconds that after MSAD-FOA optimization, the inverter stabilizes to a stable state for a very short time, and there is no overshoot phenomenon. Other algorithms cause the inverter to fail to enter the steady state in time.

In addition, as seen from Figures Fig. 13, Fig. 14 and Fig. 15, in traditional method 1, there is no online optimization of PI parameters, which causes enormous fluctuations in the frequency, voltage, and power output by the inverter, and then, the microgrid cannot work normally. In traditional method 2, PI parameters are appropriately adjusted according to human experience, but the manual adjustment accuracy is not high, especially with the increase in the number of microsources. The adjustment difficulty increases, resulting in the high-frequency oscillation of the inverter output voltage and frequency and the large-scale oscillation of the inverter output power.

The relative error of the above experiment was calculated, as shown in Table 4. Table 4 shows that the performance

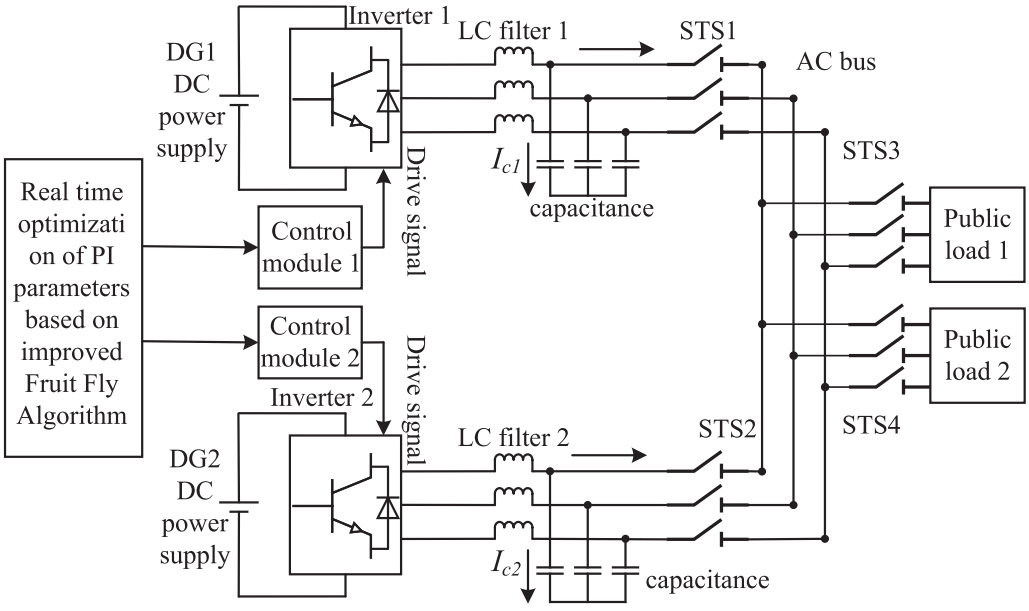

FIGURE 10. Online optimization framework of microgrid based on MSAD-FOA.

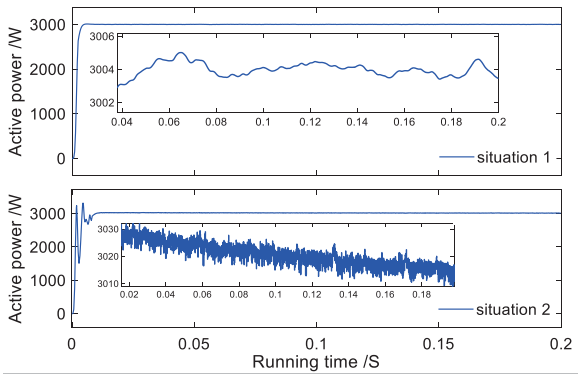

FIGURE 11. Output of active power.

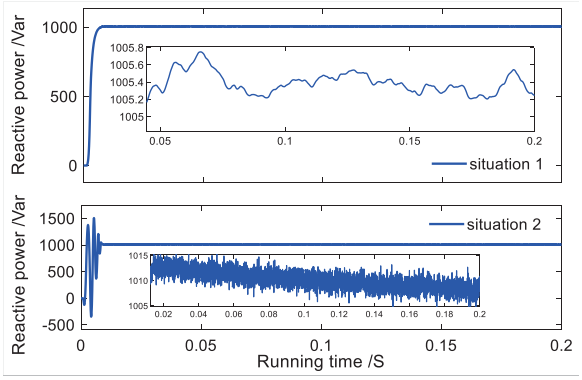

FIGURE 12. Reactive power output.

of the MSAD-FOA is slightly inferior to that of the other algorithms in terms of overshoot and is better than that of the other algorithms in terms of error and response speed. Although it is not the best algorithm in terms of overshoot, its overshoot value is very small, which meets the requirements for microgrid operation. From the perspective of steady-state time, after MSAD-FOA optimization, the system can enter a steady state in 0.005 and 0.008 seconds, which is nearly 40 times faster than other algorithms.

3) COMPARISON OF RUNNING TIME

It is difficult to design a reasonable experiment to explain the computational complexity or computational time of the algorithms. Many methods have been proposed [10], [31], [32]. A general and simple one is adopted in this paper, that is, the running time of the algorithms under the same environmental platform and the same maximum number of iterations. On the basis of comparing the convergence and diversity, the running time of each algorithm is measured simultaneously to fairly demonstrate the computational complexity of the pro-posed MSAD-FOA algorithm.

In this article's optimization strategy: All algorithms set the maximum number of iterations to 60; In the first optimization, each algorithm will give the same initial value range. The initial value range of the next optimization is determined by the optimal value of the previous optimization, this strategy is called optimal delivery strategy(ODS); The sampling time of the algorithm is 0.001 seconds. The adaptive strategy proposed in this paper can detect the environment of the algorithm, and the algorithm stops optimization when the detection environment indicators converge. For an algorithm without an adaptive strategy, the objective function F is used

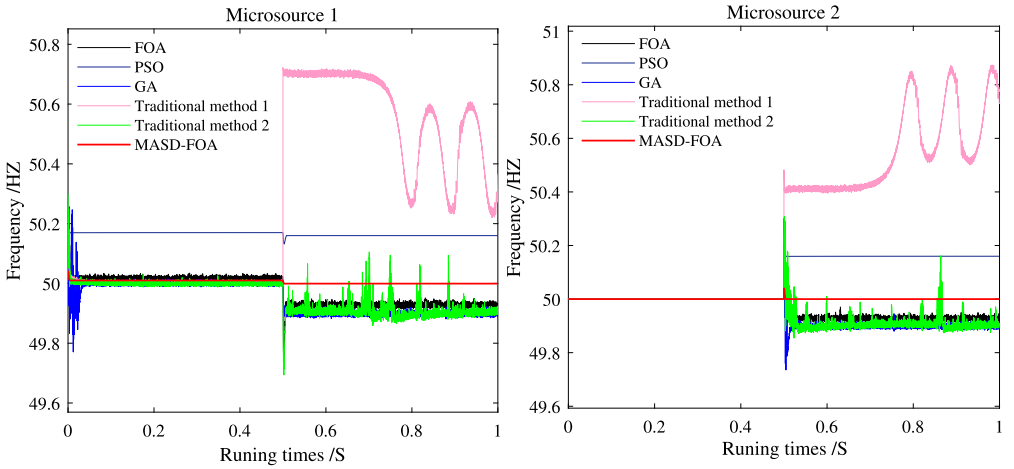

FIGURE 13. Comparison chart of inverter output frequency.

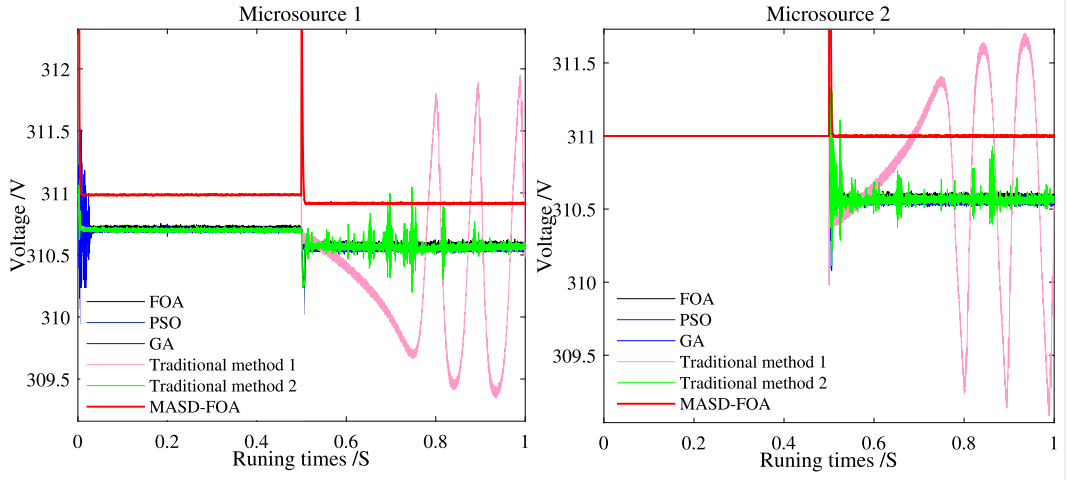

FIGURE 14. Comparison chart of inverter output voltage.

to determine whether the convergence is completed, the optimization is stopped when the convergence is completed, and the optimization is stopped when the maximum number of iterations is reached if the convergence is not completed. The comparison of different algorithms for the computational time is presented in Table 5.

It can be seen from Table 5 that the optimization strategy proposed in this paper is much shorter than other strategies in terms of optimization time, because the strategy proposed in this paper greatly reduces the number of iterations of the algorithm and makes the algorithm converge quickly. In particular, the method of determining the algorithm initial value of this time based on the optimal value of the previous time can significantly reduce the number of iterations. This is because the use of ODS can reduce the range of optimization to a certain extent, and adaptive adjustment will also intensify the convergence of the algorithm, converging rapidly in the optimal direction. Therefore, adaptive regulation strategy plays an important role in on-line optimization.

C. ANALYSIS OF ACTUAL CALCULATION EXAMPLES

1) ACTUAL EXPERIMENTAL PLATFORM

To verify the effectiveness and feasibility of the MSAD-FOA for practical applications, this article relies on the Henan Province Science and Technology Project and conducts experiments on the microgrid experimental platform of a university in Zhengzhou. The experimental environment is shown in Fig. 16.

In the experiment, monocrystalline silicon photovoltaic power generation and vertical-axis wind turbine power generation are used, the power supply is inverted according to the MSAD-FOA optimization droop control strategy, and this method is used to provide power to the load. The load adopts intelligent air conditioners and resistive load circuit (RLC) programmable load, which makes the load parameters consistent with those of the simulation experiment. The equipment parameters are as follows: the installed capacity of photovoltaic panels and wind turbines is 200 KW, the rated power of smart air conditioners is 1.18 KW (3 units), and the range of the RLC programmable load is 0:100 KW and 0:100 KVar.

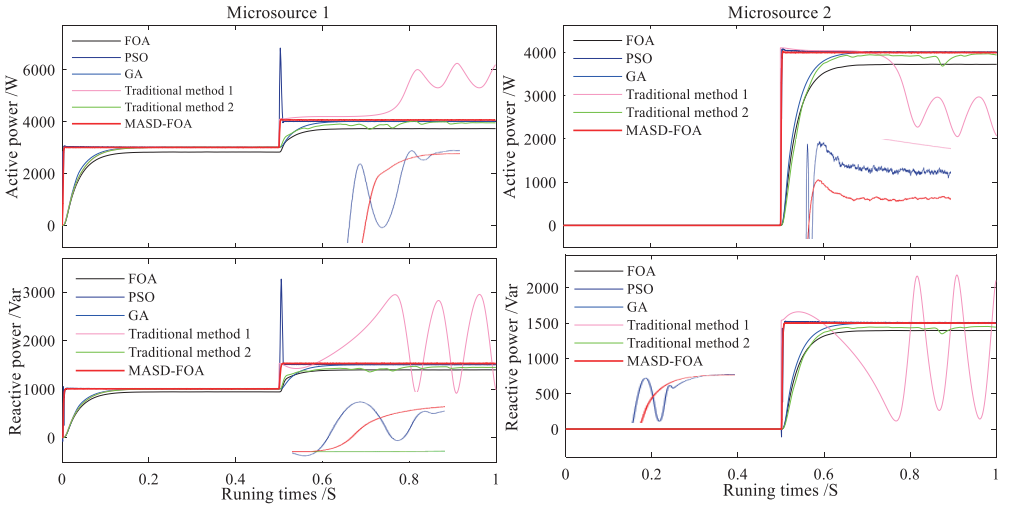

FIGURE 15. Comparison chart of inverter output power.

TABLE 4. The convergence accuracy of different algorithms and the standard deviation of the optimal value.

CA	Ms	active power power	reactive power	Frequency	Voltage	Pi1	Pi2	Over shoot	time Rise	Sst
MASD -FOA	Ms 1	1.061	1.428	5.35e-03	1.063e-01	4.554e-01	6.871e-01	1.04e+02	5e-03	5e-03
	Ms 2	2.17e-01	3.463e-01	8.681e-05	1.558e-02	4.24e-01	3.649e-01	3.3e+01	8e-03	8e-03
FOA	Ms 1	1.062e+01	1.089e+01	4.618e-02	3.513e-01	1.085e+01	6.532	0	2.35e-01	2.35e-01
	Ms 2	7.067	7.254	3.628e-02	2.077e-01	6.02	3.169	0	2.5e-01	2.5e-01
PSO	Ms 1	1.182	2.798	1.648e-01	3.784e-01	6.387e-01	8.562e-01	3.69e+03	5e-03	2.2e-01
	Ms 2	3.488e-01	6.297e-01	8e-02	2.251e-01	5.632e-01	5.424e-01	9.5e+01	5e-03	2e-01
GA	Ms 1	4.673	5.191	5.449e-02	3.764e-01	5.205	3.64	0	2e-01	2e-01
	Ms 2	3.736	3.848	5.112e-02	2.247e-01	2.241	1.421	0	2e-01	2e-01
Tm 1	Ms 1	3.123e+02	6.411e+02	1.55	5.454	2.831e+01	3.505e+01	3.028e+03	––	––
	Ms 2	9.658	9.79	2.511e-02	1.958e-01	1.032e+01	1.835	9.52e+02	––	––
Tm 2	Ms 1	7.256	7.9132	1.519e-01	5.81e-01	7.842	7.385	0	3e-01	3e-01
	Ms 2	5.618	5.869	1.256e-01	4.31e-01	6.89	6.235	0	3e-01	3e-01

[a]CA stands for Comparison Algorithm; Tm stands for Traditional method.
[b]Ms stands for microsource.
[b]Sst stands for Steady state time.

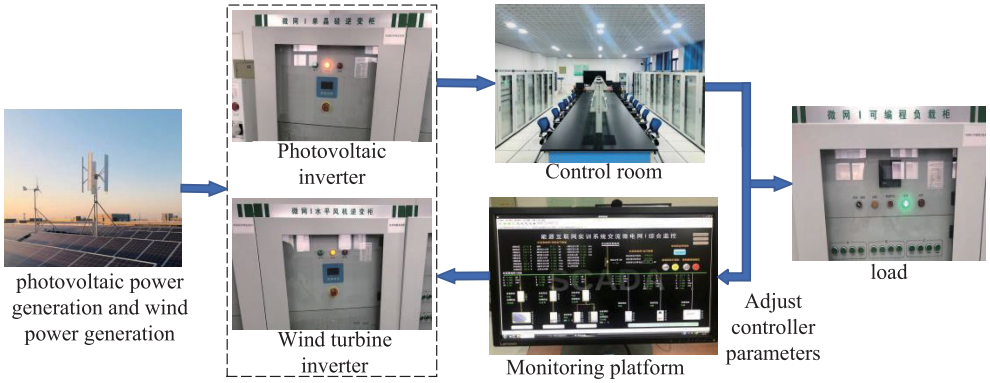

FIGURE 16. Microgrid experimental platform.

2) ACTUAL EXPERIMENTAL DESIGN

(1) Experimental environmental conditions: test time is 10:32–10:42 in the morning; outdoor temperature is 30 °C; breeze (wind speed is 5.4 m/s), sunny and cloudless.

(2) Experimental object: AC microgrid 1, solar energy and wind energy.

(3) Experimental process: before the experiment, AC microgrid 1 is separated from the system grid and

TABLE 5. Comparison of different algorithms for the computational time (all results were averaged on 30 independent runs).

	time	MSAD-FOA	FOA	PSO	GA
Number of iterations	0 S	43	60	60	60
	0.5 S	27	60	49	54
Optimization time (s)	0 S	2.15	3.00	3.00	3.00
	0.5 S	1.35	3.00	2.45	2.70

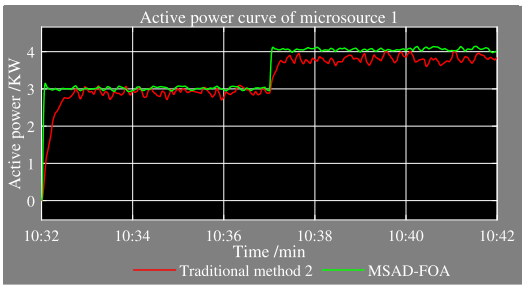

Fig. 17-(a) Active power change curve

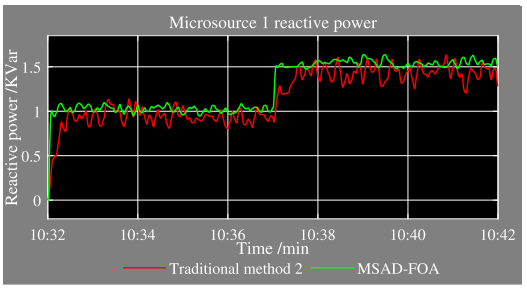

Fig. 17-(b) Variation curve of reactive power

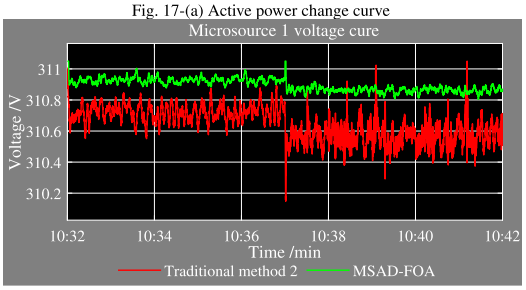

Fig. 17-(c) Voltage change curve

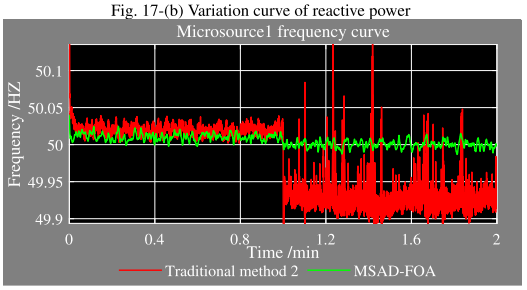

Fig. 17-(d) Frequency change curve

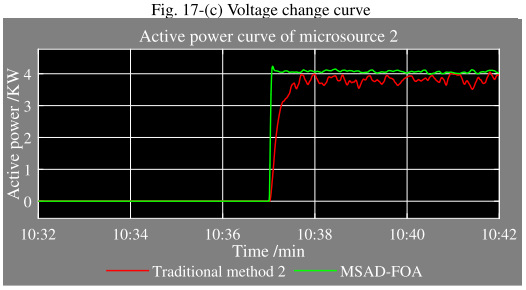

Fig. 17-(e) Active power change curve

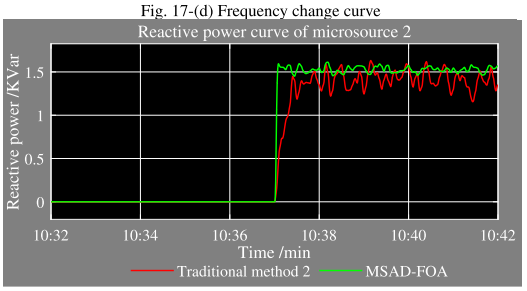

Fig. 17-(f) Variation curve of reactive power

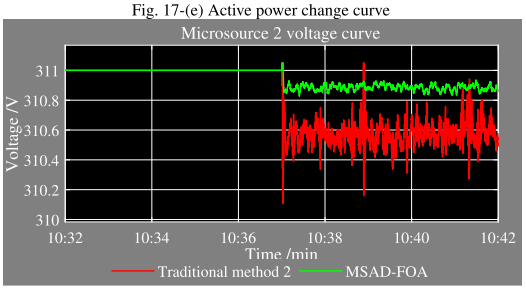

Fig. 17-(g) Voltage change curve

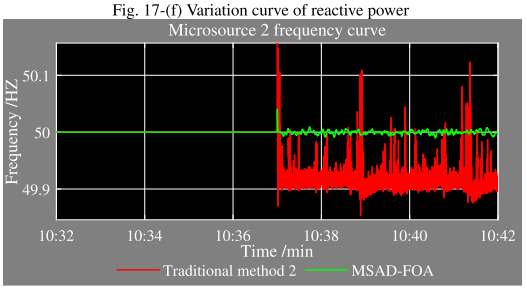

Fig. 17-(h) Frequency change curve

FIGURE 17. Experimental waveform diagram of microgrid.

operated in island mode. The monocrystalline silicon photovoltaic panel is started at 10:32, using solar power; the load is 3,000 W, 1,000 Var. The vertical-axis fan is put into operation at 10:37, using solar and wind energy to supply power at the same time, load: 8,000 W, 3,000 Var.

3) EXPERIMENTAL RESULTS AND ANALYSIS

The experimental results mainly compare the changes in the inverter output active power, reactive power, voltage and frequency during the actual operation of the microgrid. The results are shown in Fig. 17, and the analysis is as follows.

(1) When the topology and load change, the PI parameters are manually adjusted to lower the inverter output accuracy. Especially from Fig. 17-(c) and Fig. 17-(d), it can be seen that when the number of PI controls increases, manual adjustment makes the voltage and frequency oscillate, and the oscillation range is larger. However, the MSAD-FOA optimized droop control strategy makes the active power and reactive power

output by the inverter fluctuate less, the voltage and frequency be more stable, and the inverter respond faster.

(2) From Figures Fig. 17-(g) and Fig. 17-(h), it can be seen that when PI control is higher, the strategy proposed in this article can still find the best PI parameters to ensure the operation of the microgrid, so that the output of the inverter is within the allowable range.

(3) It can be seen from Fig. 17-(a), Fig. 17-(b), Fig. 17-(e) and Fig. 17-(f) that the strategy proposed in this paper makes the fluctuation range of the active power and reactive power output by the inverter smaller, and the output is more stable. The response speed is faster and better than that of traditional method 2. In summary, in the actual application process, the strategy proposed in this article is used to obtain the frequency fluctuation range of ± 0.02 Hz and the voltage fluctuation range of ± 0.12 V. The MSAD-FOA can optimize the PI parameters of the microgrid in time to ensure the stable output of the inverter.

In summary, It can be seen from the simulation verification and actual experiments that the control strategy proposed in this paper can effectively improve the output effect of the inverter. When the topology changes, MSAD-FOA will re-optimize the droop control to obtain accurate PI parameters, making the inverter's response speed faster, the error smaller, and the output more stable. During the operation of the microgrid, whether the microsource changes or the load changes, the control strategy proposed in this paper can ensure the stable output of the inverter, making the microgrid safer and more stable.

VI. CONCLUSION

An improved population division MSAD-FOA to optimize the droop control strategy is proposed in this paper and applied to an actual microgrid. This paper mainly studies the response speed, output power, voltage and frequency stability of the inverter in microgrid droop control. The main conclusions are as follows:

(1) The comparison of the MSAD-FOA with the FOA, PSO algorithm, and GA shows that the algorithm in this paper can give full play to the exploration and exploration capabilities of each fruit fly when solving different problems, so that the convergence speed and accuracy of the algorithm are improved.

(2) When the topology of the microgrid changes, the strategy proposed in this paper can optimize multiple PI parameters in parallel in the droop control of the microgrid in real time so that the robustness of the droop control is improved; the inverter responds faster, the error is smaller, and the output is more stable.

(3) The error derivation absolute value integral term is introduced into the objective function, which can effectively suppress the oscillation and offset of the inverter output power.

(4) In non-initial optimization, the combination of adaptive strategy and ODS greatly reduces the number of iterations of the algorithm, thereby reducing the time for online optimization. The comparison between the MSAD-FOA control strategy and the traditional manual adjustment of PI parameters shows that the strategy proposed in this paper also achieves better control effects in actual applications; the adjustment method is convenient, the algorithm is easy to transplant, and the promotion is strong.

Although the comprehensive researches on the optimal droop control strategy of the population division multi-strategy adaptive fruit fly algorithm have conducted in this paper, its potential is far more than that. The population division multi-strategy adaptive fruit fly algorithm can be applied to more scenarios. In the future, more attention is paid to adaptive methods. Better adaptive methods can more accurately balance the convergence and diversity of algorithms, and have achieved better optimization results. We will continue to devote ourselves to its research and improvement.

ACKNOWLEDGMENT

The authors would like to thank the anonymous reviewers and editors for their valuable suggestions and comments on the initial version of the manuscript.

COMPLIANCE WITH ETHICAL STANDARDS

CONFLICT OF INTEREST

No part of this paper has published or submitted elsewhere. The authors declare that there is no conflict of interest regarding the publication of this work.

INFORMED CONSENT

All authors have read and approve this version of the article, and due care has been taken to ensure the integrity of the work. All authors agreed to be published in IEEE ACCESS.

AUTHOR CONTRIBUTIONS

Xinkun Tao, Li Zhang and Fuzhong Wang jointly put forward the conception of this study. Xinkun Tao designed and completed the experimental studies. Both Xinkun Tao and Li Zhang participated in the analysis and interpretation of experimental results. Xinkun Tao drafted the first edition of the manuscript. Fuzhong Wang critically revised the important intellectual content of the manuscript. Xinkun Tao provided data for the experiment and modify the language of the manuscript. Xinkun Tao, Li Zhang and Fuzhong Wang approved the final version of the manuscript together.

REFERENCES

[1] Y. G. Haifeng Ling and C. Zheng, "Research on improved droop control strategy for microgrid," *Proc. CSEE*, vol. 37, no. 17, pp. 4901–4910, 2017.

[2] R.-J. Wai, Q.-Q. Zhang, and Y. Wang, "A novel voltage stabilization and power sharing control method based on virtual complex impedance for an off-grid microgrid," *IEEE Trans. Power Electron.*, vol. 34, no. 2, pp. 1863–1880, Feb. 2019.

[3] J. Z. Wenshan Li and X. Wen, "Current sharing strategy of AC/DC rectifiers based on new droop control," *Electr. Mach. Control*, vol. 24, no. 7, pp. 62–72, 2020.

[4] A. W. J. Mao and Z. Zhang, "Research on hybrid odd-order nonlinear droop control for DC microgrids based on ADRC," *High Voltage Eng.*, vol. 39, no. 2, pp. 307–314, 2018.

[5] W. Feng, W. Gao, and X. Ling, "PI parameters joint tuning for individual pitch controller of large wind turbine," *Acta Energiae Solaris Sinica*, vol. 39, no. 2, pp. 307–314, 2018.
[6] C.-T. Chen, S.-T. Peng, and C. Hwang, "A direct adaptive PI control scheme for process control," in *Proc. Eur. Control Conf. (ECC)*, Jul. 2007, pp. 5839–5844.
[7] H. Wang, M. Han, R. Han, J. M. Guerrero, and J. C. Vasquez, "A decentralized current-sharing controller endows fast transient response to parallel DC–DC converters," *IEEE Trans. Power Electron.*, vol. 33, no. 5, pp. 4362–4372, May 2018.
[8] V. Naresh Kumar and S. K. Parida, "Parameter optimization of universal droop and internal model controller for multi inverter-fed DGs based on accurate small-signal model," *IEEE Access*, vol. 7, pp. 101928–101940, 2019.
[9] T. A. Jumani, M. W. Mustafa, M. M. Rasid, N. H. Mirjat, Z. H. Leghari, and M. S. Saeed, "Optimal voltage and frequency control of an islanded microgrid using grasshopper optimization algorithm," *Energies*, vol. 11, no. 11, p. 3191, Nov. 2018.
[10] R. Dong, S. Liu, and G. Liang, "Research on control parameters for voltage source inverter output controllers of micro-grids based on the fruit fly optimization algorithm," *Appl. Sci.*, vol. 9, no. 7, p. 1327, Mar. 2019.
[11] R. Dahiya, "Distributed control for DC microgrid based on optimized droop parameters," *IETE J. Res.*, vol. 66, no. 2, pp. 192–203, Mar. 2020.
[12] M. Taghizadeh, M. Mardaneh, and M. Shasadeghi, "A new method of voltage and frequency control in isolated microgrids using enhanced droop controller optimized by frog algorithm," *J. Renew. Sustain. Energy*, vol. 6, pp. 1017–1022, Jan. 2014.
[13] P. Xie and Z. Cai, "Cooperative optimization of energy storage capacity for renewable and storage involved microgrids considering multi time scale uncertainty coupling influence," *Proc. CSEE*, vol. 39, no. 24, pp. 7126–7136, 2019.
[14] L. Wang, S. X. Lv, and Y. R. Zeng, "Literature survey of fruit fly optimization algorithm," *Control Decis.*, vol. 32, no. 7, pp. 1153–1162, 2017.
[15] G. Ding, Y. Qiao, W. Yi, W. Fang, and L. Du, "Fruit fly optimization algorithm based on a novel fluctuation model and its application in band selection for hyperspectral image," *J. Ambient Intell. Humanized Comput.*, vol. 12, no. 1, pp. 1517–1539, Jan. 2021.
[16] X. Yang, W. Li, L. Su, Y. Wang, and A. Yang, "An improved evolution fruit fly optimization algorithm and its application," *Neural Comput. Appl.*, vol. 32, no. 14, pp. 9897–9914, Jul. 2020.
[17] C. Xiong and S. Lian, "Structural damage identification based on improved fruit fly optimization algorithm," *KSCE J. Civil Eng.*, vol. 25, no. 3, pp. 985–1007, Mar. 2021.
[18] H. Chen, S. Li, A. Asghar Heidari, P. Wang, J. Li, Y. Yang, M. Wang, and C. Huang, "Efficient multi-population outpost fruit fly-driven optimizers: Framework and advances in support vector machines," *Expert Syst. Appl.*, vol. 142, Mar. 2020, Art. no. 112999.
[19] L. Lizhou and W. Youwei, "Double drive fruit fly optimization algorithm and its application in PID controller," *Control Decis.*, vol. 36, no. 9, pp. 2225–2233, 2021.
[20] Y. C. Z. Shuiping, "Fruit fly optimization algorithm for adaptive search cloud escape," *J. Huazhong Univ. Sci. Technol. (Natural Sci. Ed.)*, vol. 46, no. 9, pp. 40–44, 2018.
[21] W. Lei, X. Wensheng, Z. Liang, L. Qi, and W. Jingli, "An improved fruit fly optimization algorithm based on selecting evolutionary direction intelligently," *Int. J. Comput. Intell. Syst.*, vol. 9, no. 1, pp. 80–90, 2016.
[22] C. Xiao, K. Hao, and Y. Ding, "An improved fruit fly optimization algorithm inspired from cell communication mechanism for pre-oxidation process of carbon fiber production," in *Proc. 33rd Chin. Control Conf.*, Jul. 2014, pp. 9033–9038.
[23] L. Guoping and L. Peng, "Double strategies co-evolutionary fruit fly optimization algorithm and its application," *Comput. Integr. Manuf. Syst.*, to be published.
[24] L. Peisheng and Z. Lin, "Inverse kinematics solution of redundant manipulator based onhybrid learning fruit fly optimization algorithm," *Trans. Chin. Soc. Agricult.*, vol. 52, no. 9, pp. 410–416, 2021.
[25] L. I. Feng-yue, Q. Xiao-gang, and B. Li-ming, "Research on location-inventory joint optimization strategy based onhybrid fruit fly optimization algorithm," *Control Decis.*, to be published.
[26] X. Fu-Li and Z. Xing, "Integrated precast production scheduling and loading combinationwith considering time-varying characteristics of traffic congestion," *Comput. Integr. Manuf. Syst.*, to be published.
[27] D. Mestriner, A. Labella, M. Brignone, A. Bonfiglio, and R. Procopio, "A transient stability approach for the analysis of droop-controlled islanded microgrids," *Electric Power Syst. Res.*, vol. 187, Oct. 2020, Art. no. 106509.
[28] Q. Feng, Q. Li, W. Quan, and X.-M. Pei, "Overview of multiobjective particle swarm optimization algorithm," *Chin. J. Eng.*, vol. 43, pp. 745–753, Jun. 2021.
[29] Y. X. E. A. Tiezhou Wu and Y. Wang, "Energy optimal control strategy of HEV with PMP algorithm," *Acta Automatica Sinica*, vol. 44, no. 11, pp. 2092–2102, 2018.
[30] W.-T. Pan, "A new fruit fly optimization algorithm: Taking the financial distress model as an example," *Knowl.-Based Syst.*, vol. 26, pp. 69–74, Feb. 2012.
[31] W. Hu and G. G. Yen, "Adaptive multiobjective particle swarm optimization based on parallel cell coordinate system," *IEEE Trans. Evol. Comput.*, vol. 19, no. 1, pp. 1–18, Feb. 2015.
[32] D. Kumar and V. Kumar, "Impact of controlling parameters on the performance of MOPSO algorithm," *Proc. Comput. Sci.*, vol. 167, pp. 2132–2139, Jan. 2020.

XINKUN TAO was born in Zhengzhou, Henan, China, in 1995. He received the bachelor's degree in electrical engineering from the Zhengzhou University of Light Industry, in 2019. He is currently pursuing the master's degree in electrical engineering with the Henan University of Technology. His research interests include micro-grid optimization control and intelligent algorithm design. He has published three high-level papers during the post-graduate period, won honors such as the school's special scholarship, and outstanding graduate student.

LI ZHANG was born in Linfen, Shanxi, China, in 1982. She received the bachelor's and master's degrees in control engineering from the Henan University of Technology, in 2005 and 2008, respectively, and the Ph.D. degree from Wuhan University, in 2016. She is currently a Master Instructor with China Henan Polytechnic University. She has published more than 20 high-level papers, presided over and participated in more than ten major research and exploration projects. Her research interests include smart grid demand-side management and smart power consumption information processing.

FUZHONG WANG was born in Mengzhou, Henan, China, in 1962. He is currently a Ph.D. Tutor with China Henan Polytechnic University. He has published more than 100 high-level papers, presided over and participated in more than 20 major research and exploration projects. His research interests include power system optimization and control, artificial intelligence control, intelligent information processing, and fault diagnosis.